Article **Journal-Mathematical and Quantitative Methods**
December 2021, Vol.5 No.9 25-34

Steady-state simulation model of a smart load based on the electric spring implemented in Simulink

Modelo de simulación en estado estable de una carga inteligente basada en el resorte eléctrico implementado en Simulink

RICO-VELA, José Luis*†´, TAPIA-TINOCO, Guillermo´´, FIGUEROA-GODOY, Fernando´´ and LOZANO-LUNA, Alfonso´´

´Instituto Tecnológico Superior de Irapuato, Electromechanical Engineering, Irapuato, Mexico.
´´ Tecnológico Superior de Irapuato, Electromechanical Engineering, Irapuato, Mexico.

ID 1st Author: *José Luis, Rico-Vela*

ID 1st Co-author: *Guillermo, Tapia-Tinoco*

ID 2nd Co-author: *Fernando, Figueroa-Godoy*

ID 3rd Co-author: *Alfonso, Lozano-Luna*

DOI: 10.35429/JMQM.2021.9.5.25.34 Received July 30, 2021; Accepted December 30, 2021

Abstract

The Smart load simulation model based on the electric spring operation principle is presented. The proposed simulation model is implemented in the numerical software Simulink of Matlab and it is useful for the state stable analysis of the smart load. Proposal simulations show the effectiveness of the smart load to modify the power factor through of inductive, capacitive, active and complex power compensation.

Model, Simulation, Simulink

Resumen

En este trabajo se presenta el modelo de simulación de una carga inteligente basada en el principio de funcionamiento del resorte eléctrico. El modelo de simulación propuesto se implementa en Simulink de Matlab y es útil para el análisis en estado estable de la carga inteligente. Con los casos de estudio propuestos se muestra la efectividad de la carga inteligente para modificar el factor de potencia mediante la compensación de potencia inductiva, capacitiva, real y compleja.

Modelo, Simulación, Simulink

Citation: RICO-VELA, José Luis, TAPIA-TINOCO, Guillermo, FIGUEROA-GODOY, Fernando and LOZANO-LUNA, Alfonso. Steady-state simulation model of a smart load based on the electric spring implemented in Simulink. Journal-Mathematical and Quantitative Methods. 2021. 5-9:25-34.

† Researcher contributing as first author.

© RINOE–Spain

Introduction

Due to the stochastic nature of alternative energy sources and the large number of large-scale and small-scale power plants that will be built in the coming years as a result of the measures adopted by different countries with the purpose of improving the environment and creating sustainable development [1]- [4], the current control of power generated according to demand is not viable, causing instability in the current power system [5]. Due to this reason, smart grids with high penetration of renewable energy sources require solving a new control paradigm, which establishes that the system responds in real time allowing the generated power to follow the demand [6], within the specified operation and control limits. In the literature there are reported control techniques based on the measurement of the demanded load in time lapses of days or hours [7]-[9], use of energy storage to alleviate peak demand [10] and on-off control of smart loads [11]-[13], the first two of them cannot respond to power fluctuations in real time and the third one causes too much inconvenience to the consumer. In more recent research, a new smart load scheme based on electric spring has been proposed, which has been shown theoretically and practically in [14]-[17].

In these contributions, the working principle of the smart load, its control stages and the implementation of the smart load are shown. In addition, case studies that allow observing the behavior of the intelligent load for voltage control in single-phase power systems with high penetration of alternate energy sources are presented experimentally.

Returning to the principle of operation and the mathematical modeling presented in [16], in this work a simulation model of the intelligent load is proposed, this mathematical model is suitable for steady state analysis of the intelligent load and presents a useful tool for the interaction of the intelligent load with a power system.

Steady-state operating principle of the electric spring

Figure 1 is used to show the steady-state operating principle of the smart load when connected to a power system represented by the voltage source VF. The smart load consists of the electric spring VRE and a noncritical impedance Z.

The electric spring is modeled as an AC voltage source whose magnitude and phase angle can be controlled. The noncritical load can operate with unity power factor, forward or backward. Equation (1) corresponds to the complex power of each of the elements in Figure 1, with (SF, SZ, SRE), (PF, PZ and PRE) and (QF, QZ and QRE) being the complex, real and reactive powers of the source, non-critical load and electric spring respectively, while (θs, βs, Φs) is the power factor angle of each element. Equation (2) is obtained by performing power balance in the circuit and the signs (+,-) are associated with power consumption and power generation respectively.

The electric spring operates in eight different operating modes: inductive power compensation (+jQRE), capacitive power compensation (-jQRE), positive real power compensation (+PRE), negative real power compensation (-PRE), inductive and positive real power compensation.

(+jQRE and +PRE), negative inductive and real power compensation (+jQRE, - PRE), positive capacitive and real power compensation (-jQRE, +PRE) and negative capacitive and real power compensation (-jQRE, -PRE) [16].

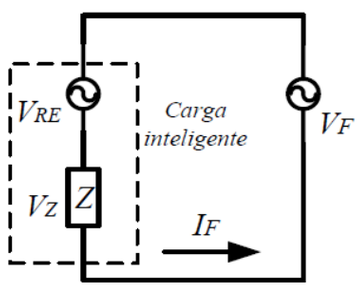

Figure 1 Schematic representation of the electric spring

ISSN-On line: 2531-2979
RINOE® All rights reserved.

$$\begin{aligned} |S_F|\angle\theta_S &= \pm P_F \pm jQ_F \\ |S_Z|\angle\beta_S &= \pm P_Z \pm jQ_Z \\ |S_{RE}|\angle\Phi_S &= \pm P_{RE} \pm jQ_{RE} \end{aligned} \quad (1)$$

$$\begin{aligned} \pm P_F &= \pm P_{RE} \pm P_Z \\ \pm jQ_F &= \pm jQ_{RE} \pm jQ_Z \end{aligned} \quad (2)$$

Figure 2 shows the phasor diagrams illustrating the eight modes of operation of the electric spring. In all cases presented the VF source operates with unity power factor and the real and reactive power compensation is performed by the electric spring. Figure 2(a) corresponds to the inductive power compensation (+jQRE). It can be seen that in this mode of operation the real power consumed by the load is supplied by the source, while the reactive generated by the load are consumed by the electric spring.

Figure 2(b) corresponds to capacitive compensation, in this mode of operation the electric spring injects reactants (-jQRE). As seen in the phasor diagram the load is RL, therefore it consumes real power which is provided by the source and the reactants which are provided by the electric spring.

Figures 2(c) and 2(d) correspond to the positive (+PRE) and negative (-PRE) real power compensation mode of operation respectively. In the case of (+PRE) the electric spring consumes power, therefore the source must provide the power consumed by the load and the electric spring. However in (-PRE) the electric spring injects power, causing part of the power to be consumed by the load:

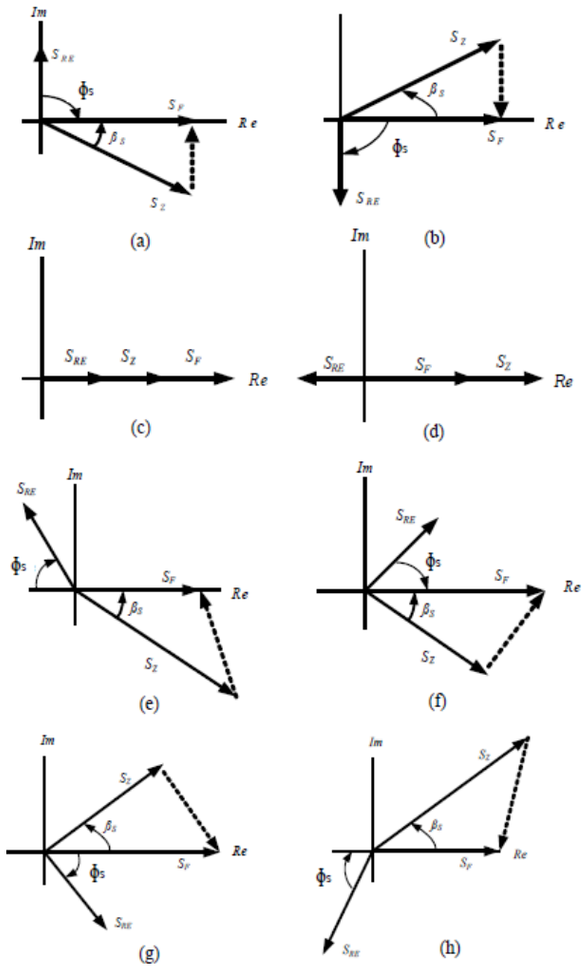

Figure 2 Intelligent load operating modes. a).-. (+jQRE), b).- (-jQRE), c).- (+PRE), d).- (-PRE), e).- (+jQRE, -PRE), f).- (+jQRE and +PRE), g).- (-jQRE, +PRE), h).- (-jQRE, +PRE), h). jQRE, -PRE)

Consumed by the load is contributed by the electric spring. Figure 2(e) shows the mode of operation of the electric spring with inductive and real power compensation positive (+jQRE and +PRE).

In this mode of operation the electric spring consumes real and reactive power, the real power being provided by the source and the reactive power by the load. Figure 2(e) shows the case in which the electric spring consumes reactive power and injects real power (+jQRE, -PRE).

For the capacitive compensation mode of operation, equation (3) is used to calculate IS, however the voltage is calculated with (5), which differs from (4) because now the angle of the electric spring is -π/2.

ISSN-On line: 2531-2979
RINOE® All rights reserved.

Figure 2(f) shows the capacitive and positive real power compensation mode of operation (-jQRE, +PRE). In this mode the electric spring injects reactive power and consumes reactive power. Finally the (-jQRE, -PRE) mode, in this mode the electric spring injects both real and reactive power, i.e. the reactive power consumed by the load is provided by the electric spring and part of the real power consumed by the load.

Mathematical Formulation

In [16] the mathematical formulation for calculating the steady-state voltage magnitude and phase angle of the electric spring according to the mode of operation in which it is required to operate is reported.

To operate in inductive compensation mode, equations (3) and (4) are used. In this mode of operation the electric spring is seen by the system as an inductor since it consumes reactants. First, with (3) the source current is determined and with (4) the magnitude of the electric spring voltage is determined. The phase angle of the electric spring voltage must be π/2.

$$I_F \angle \theta_I = \frac{V_F}{R} \angle 0 \quad (3)$$

$$V_{RE} \angle \theta_v = XIs \angle \frac{\pi}{2} \quad (4)$$

Where:

VF source voltage

IF source current.

θI phase angle of the source current.

R load resistance.

VRE magnitude of electric spring voltage.

θv phase angle of the load voltage.

X load reactance.

$$V_{RE} \angle \theta_v = XIs \angle -\frac{\pi}{2} \quad (5)$$

Equations (6) and (7) are used to determine the voltage and phase angle of the electric spring to operate in positive real power mode of operation (Sz < SF), while (6) and (8) are used in negative power mode of operation (Sz > SF). In both cases initially the power to be injected by the source is calculated and subsequently the electric spring voltage is calculated.

$$I_s = \angle \theta_I = \frac{P_F}{V_F} \angle 0 \quad (6)$$

$$V_{RE} \angle \varphi_V = V_F - I_F R \angle 0 \quad (7)$$

$$V_{RE} \angle \varphi_V = I_F R - V_F \angle \pi$$

Where:

φv phase angle of the electric spring voltage.

If complex power compensation is required, equations (9), (10) and (11) are used. These equations allow calculating the voltage and phase angle of the electric spring to perform the change from an initial complex power PF1, QF1 (without electric spring) to a final power PF2, QF2 (with electric spring). They can also be used when you want to perform real power compensation (PF1 to PF2) keeping constant reactive power (QF1=QF2) or reactive power compensation (QF1 to QF2) keeping constant real power (PF1 = PF2).

$$I_{F2} \angle \theta_{I2} = \frac{\sqrt{P_{F2}^2 + Q_{F2}^2}}{V_F} \angle -\arctan\left(\frac{Q_{F2}}{P_{F2}}\right) \quad (9)$$

$$V_{s2} \angle \theta_{V2} = V_F \sqrt{\frac{P_{F2}^2 + Q_{F2}^2}{P_{F1}^2 + Q_{F1}^2}} \angle \left[\arctan\left(\frac{Q_{F1}}{P_{F1}}\right) - \arctan\left(\frac{Q_{F2}}{P_{F2}}\right)\right] \quad (10)$$

$$V_{RE} \angle \varphi_V = V_s \angle 0 - V_{o2} \angle \theta_{V2} \quad (11)$$

Simulation Model

Figure 3 shows the simulation model implemented in Simulink which corresponds to a single-phase power system. The system has the circuit topology of Figure 1. The voltage source (VF), the electric spring (VRE) and the non-critical load Z are connected in series. In addition, the "graph" blocks the "plotter" and "display" blocks and the display" blocks and the subsystems "measurements", "signals" and "measurements", "signals" and "power" subsystems.

ISSN-On line: 2531-2979
RINOE® All rights reserved.

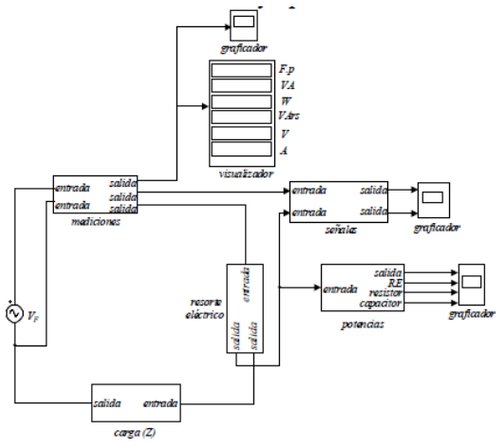

Figure 3 Simulation model

The "plotter" and "display" blocks allow to observe graphically and numerically the voltage, current, power factor and power signals of the VF source. The "measurements" subsystem allows to measure the voltage and current in each of the elements of the power system. The "signals" subsystem allows visualizing the behavior over time of the voltages and currents of each element.

Finally, the power subsystem is used to calculate the real, reactive and apparent power of each element of the power system.

Case Studies

The purpose of the case studies is to validate the simulation model with the eight modes of operation of the electric spring and the equations shown in the mathematical formulation section. Five case studies are presented. In the first two, inductive and capacitive inductive and capacitive compensation respectively, the third case shows the electric spring operating in the third case shows the electric spring operating in positive and negative real power and negative real power mode. In the last two cases of study, the electric spring performs the complex power complex power compensation, for which in the fourth in the fourth case of study, the reactive power is kept constant and the reactive power is kept constant and the real power is real power is modified, while in the last case study, the real power is the real power is kept constant and the reactive power is the reactive power is modified.

The parameters used in the simulation are shown in Table 1. VF is kept at 110 VRMS and with a frequency of 60 Hz. Z can be R, RL or RC depending on the case of study and the magnitudes are as shown in the table. The magnitude and phase angle of the electric spring are calculated with equations (3)-(11) according to the type of compensation.

In each case of study, the instantaneous voltages of the source (VF), the electric spring (VRE) and the Z load (VR, VC and VL) are presented, in addition to the current delivered by the source (IF), which is multiplied by a factor of 20 for better visualization of 20 for better visualization. Additionally, the voltage, current, power and power factor at which VF operates with the electric spring and without the electric spring are compiled in a table.

	Parámetro	Magnitud
Fuente de voltaje	V_F	$110V_{RMS}$ @60Hz
Carga	Z	R: 55 Ω RC: 52-38jΩ RL: 56 + 40jΩ
Resorte eléctrico	V_{RE}	Dependiendo el caso

Table 1 Simulation Parameters

Inductive power compensation.- In this case study the load Z = (52- 38j)Ω is used. 2 0o F I and 76 90o RE V are calculated with equations (3) and (4) respectively.

Figure 4(a) shows the voltages and current without the electric spring. It can be clearly observed that the voltage source operates with a different power factor than unity since IF overtakesVF, which is due to the type of load (RC). Figure 4(b) shows the operation of the electric spring in inductive mode, which is due to the type of load (RC).

This is determined by the phase angle between VRE and IF, which is 90o in retardation.

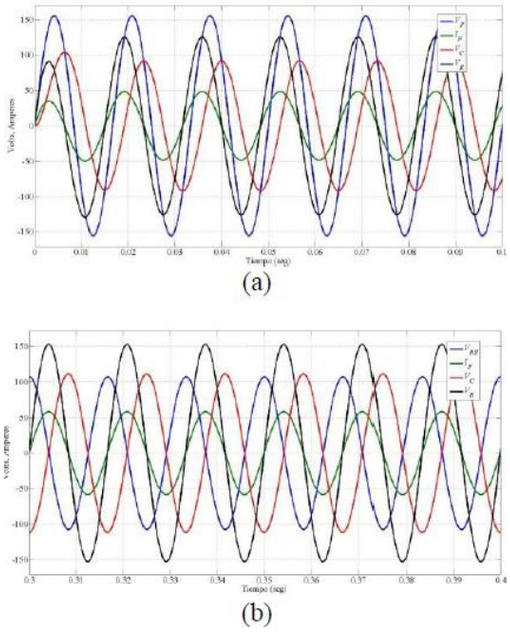

Figure 4 Inductive compensation +jQRE. a).- Without electric spring, b).- With electric spring.

Table 2 shows the conditions at which VF operated without the electric spring and how it modifies the power factor and consequently the reactive power when the electric spring is included. The P.F. is close to unity which is due to the fact that the reactive power delivered by the load is consumed by the electric spring.

	Sin resorte eléctrico	Con resorte eléctrico
F.P	+ 0.8074	+ 0.996
S_F	187.8 VA	228.4 VA
P_F	151.7 W	228.3 W
Q_F	110.8 Vars	6.044Vars
V_F	110 V	110 V
I_F	1.708 A	2.076 A

Table 2 Operation mode +jQRE

Capacitive compensation - In this case study the load Z = 56+40jΩ is used. Equations (3) and (5) are used to achieve the compensation and VF to operate with unity power factor, giving as a result 2 0o FI and 76 90o REV. Figure 5 shows the waveforms of the voltages and current with and without the electric spring.

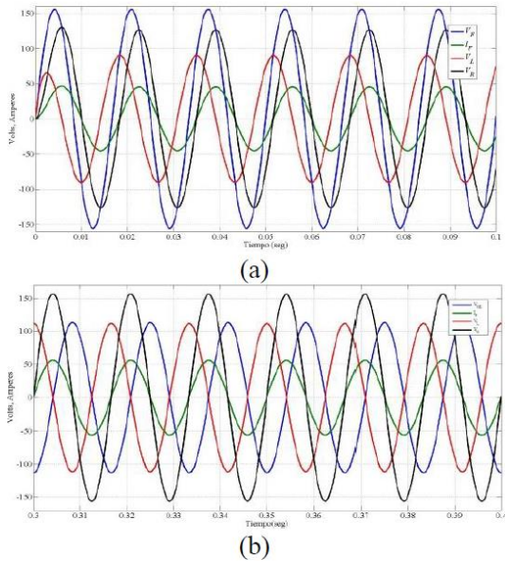

Figure 5 Capacitive compensation -jQRE. a).- Without electric spring, b).- Without electric spring, c).- Without electric spring, d). b).- With electric spring

It is clearly seen in Figure 5(a) that by not including the electric spring the current IF lags the voltage due to the load RL. On the other hand, in Figure 5(b) the electric spring operates in capacitive operation mode since IF is 90º ahead of VRE. Table 3 clearly shows the P.F correction made by the electric spring as the reactive power delivered by VF is close to zero. This is due to the fact that the reactive power consumed by VF is close to zero.

Because the reactive power consumed by the load is provided by the spring. is provided by the electric spring.

	Sin resorte eléctrico	Con resorte eléctrico
F.P	- 0.8137	-1
S_F	175.8 VA	217.4 VA
P_F	143.1W	217.4 W
Q_F	102.2 Vars	1.86 Vars
V_F	110 V	110 V
I_F	1.598 A	1.976 A

Table 3 Mode of operation -jQRE

Positive and negative real power compensation.- A purely resistive load Z= 55Ω is used for this case study. Figure 6(a) shows the voltages and current without the electric spring, it can be observed that they are in phase and VF = VR are in phase and VF = VR. Figure 6(b) shows the results operating the electric spring in positive real power mode.

To achieve such mode of operation, it is considered that the source provides a power PF = 180 W and with equations (6) and (7) we obtain 1.636 0o F I and 20.02 0o RE V. Figure 6(c) presents the results when the electric spring operates in negative real power compensation mode. To to achieve this mode of operation VRE must maintain an offset with IF of 180º as shown in the figure. In this mode of operation PF = 270 W is considered and with equations (7) and (8) we calculate 2.454 0o F I and 25 180 RE V. Without electric spring the power at the load PZ = 220 W, in positive real compensation mode PZ = 147.2 W and in negative real operation mode PZ = 331.4W.

The results reported in Table 4 show how in all cases the unit power factor is operated with a unity power factor

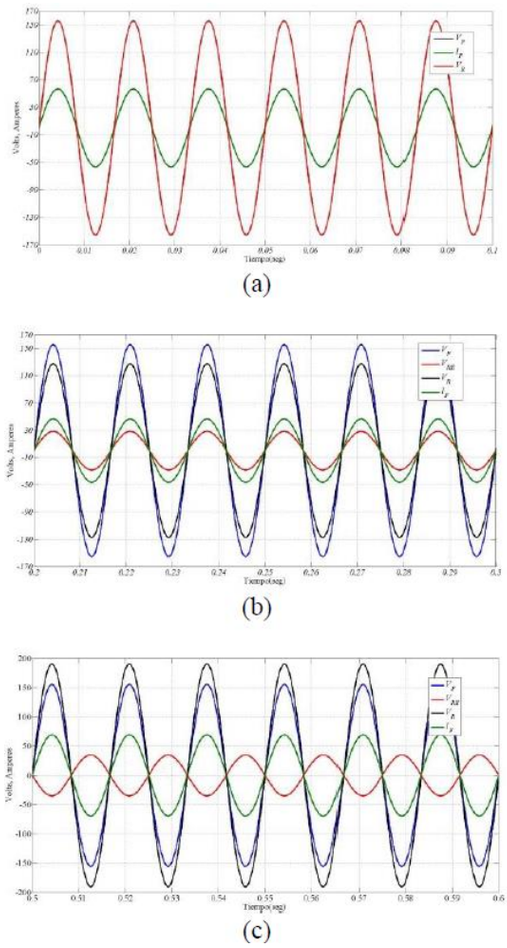

Figure 6 Real power compensation a).- Without electric spring, b).- With electric spring, c).- With electric spring, d). b).- With electric spring +PRE, b).- Without electric spring -PRE, c).- With electric spring +PRE, d). electric spring -PRE

In addition, in the positive real power compensation mode positive real power compensation mode PF>PZ, while in negative real power compensation mode PF<PZ PF<PZ, this is due to the fact that part of the power that part of the power consumed by the load is provided by the electric spring. is provided by the electric spring.

	Sin resorte eléctrico	Potencia real positiva	Potencia real negativa
F.P	1	1	1
S_F	220 VA	180 VA	270 VA
P_F	220 W	180 W	270 W
Q_F	0 Vars	0 Vars	0 Vars
V_F	110 V	110 V	110 V
I_F	2 A	1.637 A	2.48 A

Table 4 Power Compensation +PRE, PRE

Complex power compensation with constant real power - In this case study the appropriate voltage and phase angle are calculated to perform the complex power compensation keeping constant the real power delivered by the electric spring.

For this case study a load RL with values Z = 56+40j Ω is considered. Without the electric spring VF operates with a power factor of 0.814 in lagging which corresponds to PF =143.13 W and QF =102.2 VAR, Figure 7(a) shows the voltages and currents without the electric spring. Figure 7(b) is divided into two periods, the first period being at $0.1 \leq t < 0.2$ sec. In this period the electric spring performs the compensation of positive real power and inductive power as it changes the source power factor from 0.814 to 0.7. To carry out the change in the power factor, equations (9)- (11) are used with the values PF = 143.13W, QS1=102.2 VAR and QS2=146.02 VAR, giving as a result 2 1.859 45.57 o FI , 2127.89 10.04 o Z V and 27.4 125.55 o RE V.

Subsequently at $t \geq 0.2$ sec the electric spring voltage takes a new value to modify the power factor to 0.9, therefore the electric spring will perform positive real power and capacitive power compensation. The theoretical values of power delivered by the source are PF = 143.13W, QS1=102.2 VAR and QS2=69.32 VAR, giving as a result when substituting in equations (9)-(11) 2 1.446 25.84 FI, 299.47 9.69 ZV 20.57 54.48 REV.

When analyzing the figures, the operation of the electric spring is the operation of the electric spring is clearly observed when it performs the compensation of real and inductive power IF real and inductive power compensation lags VRE, however, when performing real and capacitive real and capacitive compensation IF advances VRE. Table 5 shows how voltage source operates with different power factors power factors, all of them being lagging power factors. power factors in backward. It can also be seen that the theoretical values used to calculate the electric spring voltage are voltage of the electric spring are very close to those obtained by those obtained by simulation.

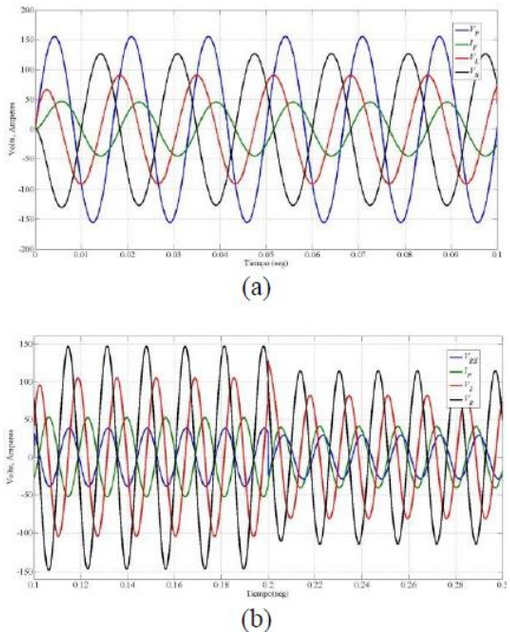

Figure 7 Complex power compensation a).- Without electric spring, b).- +PRE fixed and +QRE to -QRE rafter.

	Sin resorte eléctrico	Con resorte eléctrico,	Con resorte eléctrico,
F.P	-0.8137	-0.7	-0.9
S_F	175.8 VA	204.4 VA	159 VA
P_F	143.1 W	143.1 W	143.1 W
Q_F	102.2 Vars	146 Vars	69.31 Vars
V_F	110 V	110 V	110 V
I_F	1.598 A	1.858 A	1.445 A

Table 5 Complex power compensation with fixed +PRE and switching from +QRE to -QRE

Complex power compensation with constant reactive power

In this case study the appropriate voltage and phase angle are calculated to perform the complex power compensation keeping constant the reactive power delivered by the electric spring. For this case study an RC load with Z = 52-38j Ω values is considered.

Without the electric spring VF operates with a power factor of 0.807 in forward which corresponds to PF = 151.7 W and QF = -110.9 VAR, Figure 8(a) shows the voltages and currents without the electric spring. Figure 8(b) is divided into two periods, the first period being at $0.1 \leq t < 0.2$ sec. In this period the electric spring changes the F.P from 0.814 to 0.7. To carry out the change in the power factor, equations (9)- (11) are used with the values QF = -110.9 VAR, PS1=151.7 W and PS2=108.7 W, resulting in 2 1.412 45.57 or FI, 2 90.9 9.40 or ZV and 25.17 36.15 or REV.

Subsequently at $t \geq 2$ sec the electric spring voltage changes to modify the power factor to 0.9. The theoretical values of power delivered by the source are QF = -110.9 VAR, PS1=151.7 W and PS2=228.98 W, resulting when substituting in equations (9)-(11) 2 2.31 25.84 or FI, 2 148.93 10.33 or ZV and 45.24 10.33.

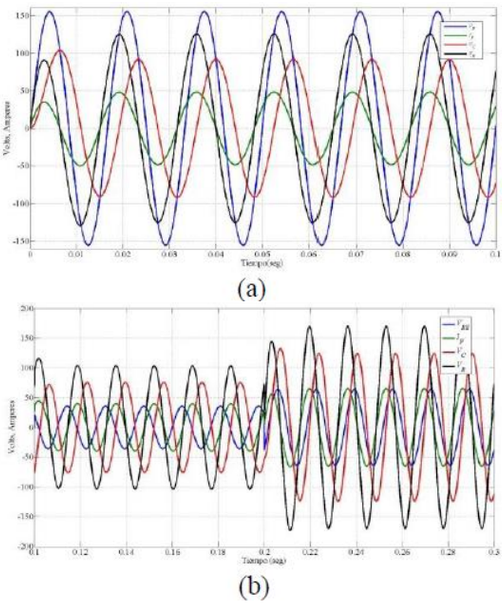

Figure 8 Complex power compensation a).- No electric spring, b).- +QRE fixed and +PRE change

When analyzing VRE and IF in Figure 8(b) it is clearly observed how the electric spring changes from a lagging power factor to a leading power factor, this with the purpose of modifying the P.F. of VF without modifying the reactive power consumed by the power consumed by the electric spring. Table 6 shows how the voltage source voltage source operates with the different power factors, all of them being power factors, all of them being forward power factors.

ISSN-On line: 2531-2979
RINOE® All rights reserved.

Power factors in advance. In addition, it can be seen that the theoretical values of power and power factor of VF used to calculate the voltage VF power factor used to calculate the electric spring voltage are very close to those obtained by simulation. obtained by simulation.

	Sin resorte eléctrico	Con resorte eléctrico,	Con resorte eléctrico,
F.P	0.8074	0.7002	0.9002
S_F	187.9 VA	152.2 VA	255.3 VA
P_F	151.7 W	108.7 W	229.9 W
Q_F	-110.8 Vars	-110.8 Vars	-110.8 Vars
V_F	110 V	110 V	110 V
I_F	1.708 A	1.411 A	2.32 A

Table 6 Complex power compensation with +QRE and +PRE switching

Conclusions

The case studies shown in this work allow corroborating the principle of operation of the smart load and its mathematical foundation. The different modes of operation of the smart load were shown in the case studies.

The results obtained in the simulations are very close to those calculated theoretically and those reported in the literature. On the other hand, the simulation model and the mathematical formulation together present a useful tool for the steady state analysis of power systems, allowing the study of intelligent loads in more complex power systems.

References

20% Wind Energy by 2030, U.S. Department of Energy, 2008.

Meeting the Energy Challenge A White Paper on Energy, Department of Trade and Industry, 2007 The European Strategic Energy Technology Plan SET- Plan Towards a low- carbón future, European Commission, 2010.

(2014) Página de internet SENER RENOVABLES. [Online]. Disponible http://www.renovables.gob.mx

P. Gopakumar, M. J. Reddy and D. K. Mohanta, "Stability Concerns in Smart Grid with Emerging Renewable Energy Technologies", Electric Power Components and Systems, Vol. 42(3-4), pp. 418-425, February 2014.

M. E. El-hawary, "The Smart Grid-State-of-the-art and Future Trends", Electric Power Components and Systems, Vol. 42(3-4), pp. 239-250, February 2014.

A. Mohsenian-Rad, V. W. S. Wong, J. Jatskevich, R. Schober, and A. Leon-Garcia, "Autonomous demand-side management based on gametheoretic energy consumption scheduling for the future Smart grid," IEEE Trans. Smart Grid, vol. 1, no. 3, pp. 320–331, 2010.

M. Parvania and M. Fotuhi-Firuzabad, "Demand response scheduling by stochastic SCUC," IEEE Trans. Smart Grid, vol. 1, no. 1, pp. 89–98, 2010. M. Pedrasa, T. D. Spooner, and I. F. MacGill, "Scheduling of demand side resources using binary particle swarm optimization," IEEE Trans. Power Syst., vol. 24, no. 3, pp. 1173–1181, 2009.

F. Kienzle, P. Ahc in, and G. Andersson, "Valuing investments in multi-energy conversion, storage, and demand-side management systems under uncertainty," IEEE Trans. Sustainable Energy, vol. 2,no. 2, pp. 194–202, 2011.

S. C. Lee, S. J. Kim, and S. H. Kim, "Demand side management with air conditioner loads based on the queuing system model," IEEE Trans. Power Syst., vol. 26, no. 2, pp. 661–668, 2011.

G. C. Heffner, C. A. Goldman, and M. M. Moezzi, "Innovative approaches to verifying demand response of water heater load control,"IEEE Trans. Power Delivery, vol. 21, no. 1, pp. 388–397, 2006.

A. Brooks, E. Lu, D. Reicher, C. Spirakis, and B. Weihl, "Demand dispatch," IEEE Power Energy Mag., vol. 8, no. 3, pp. 20–29, 2010.

C.K. Lee, N. R. Chaudhuri, B. Chaudhuri and S.Y.R. Hui, "Droop Control of Distributed Electric Springs for Stabilizing Future Power Grid", IEEE Transaction on Smart Grid, Vol. 4, No. 3, September 2013.

C. K. Lee and S.Y.R. Hui, "Reduction of Energy Storage Requirements in Future Smart Grid Using Electric Spring", IEEE Transaction on Smart Grid, Vol. 4, No. 3, September 2013

ISSN-On line: 2531-2979
RINOE® All rights reserved.

S. Chong Tan, Chi K. Lee and S. Y. Ron Hui, "General Steady-State Analysis and Control Principle of Electric Springs With Active and Reactive Power Compensations", IEEE Transactionson on Power Electronics, Vol. 28, No. 8, pp. 3958-3969, August 2013.

C. K. Lee, B. Chaudhuri and S. Y. Hui, "Hardware and Control Implementation of Electric Springs for Stabilizing Future Smart Grid With Intermittent Renewable Energy Sources" IEEE Journal of Emerging and SelectedTopics in PowerElectronics, Vol. 1, No. 1, March 2013.

ISSN-On line: 2531-2979
RINOE® All rights reserved.